Microsc. Microanal. 21, 753–758, 2015
doi:10.1017/S1431927615000495

Microscopy AND Microanalysis

© MICROSCOPY SOCIETY OF AMERICA 2015

Monte Carlo Simulation of Characteristic Secondary Fluorescence in Electron Probe Microanalysis of Homogeneous Samples Using the Splitting Technique

Mauricio Petaccia,[1,2] Silvina Segui,[3,4] and Gustavo Castellano[1,2,*]

[1]*FaMAF, Universidad Nacional de Córdoba, Medina Allende s/n, Ciudad Universitaria, 5000 Córdoba, Argentina*
[2]*Instituto de Física Enrique Gaviola (IFEG), 5000 Córdoba, Argentina*
[3]*Centro Atómico Bariloche, Comisión Nacional de Energía Atómica, Avenida Bustillo 9500, 8400 S.C. de Bariloche, Río Negro, Argentina*
[4]*CONICET, Av. Rivadavia 1917, C1033AAJ Buenos Aires, Argentina*

Abstract: Electron probe microanalysis (EPMA) is based on the comparison of characteristic intensities induced by monoenergetic electrons. When the electron beam ionizes inner atomic shells and these ionizations cause the emission of characteristic X-rays, secondary fluorescence can occur, originating from ionizations induced by X-ray photons produced by the primary electron interactions. As detectors are unable to distinguish the origin of these characteristic X-rays, Monte Carlo simulation of radiation transport becomes a determinant tool in the study of this fluorescence enhancement. In this work, characteristic secondary fluorescence enhancement in EPMA has been studied by using the splitting routines offered by PENELOPE 2008 as a variance reduction alternative. This approach is controlled by a single parameter NSPLIT, which represents the desired number of X-ray photon replicas. The dependence of the uncertainties associated with secondary intensities on NSPLIT was studied as a function of the accelerating voltage and the sample composition in a simple binary alloy in which this effect becomes relevant. The achieved efficiencies for the simulated secondary intensities bear a remarkable improvement when increasing the NSPLIT parameter; although in most cases an NSPLIT value of 100 is sufficient, some less likely enhancements may require stronger splitting in order to increase the efficiency associated with the simulation of secondary intensities.

Key words: EPMA, characteristic fluorescence enhancement, Monte Carlo simulation, variance reduction

Introduction

Electron probe microanalysis (EPMA) is a powerful analytical tool, which allows chemical quantification of the elements present in samples of different characteristics, along a wide range of specimen compositions. When a finely collimated electron beam impinges on a flat material, the characteristic intensity emitted by each element composing the sample can be used not only to identify these elements, but they may be recorded and then compared with the corresponding intensities emitted from standards of known composition. This comparison originates in the assumption that the emitted characteristic intensities proportionally relate to the mass concentrations of the corresponding elements, which allows to eliminate geometrical and physical factors that are very difficult to determine (Reed, 1993; Scott et al., 1995). With adequate procedures for data reduction, the different matrix effects are taken into account, usually referred to as "*ZAF* correction" (Goldstein et al., 2003); also called "matrix corrections," they were originally separated into factors accounting for differences in the generation of X-rays and scattering of the incident beam (*Z*, for atomic number correction), absorption effects (*A*), and secondary fluorescence enhancement (*F*). These matrix correction factors strongly depend on the experimental conditions, mainly on the incident beam energy, X-ray take-off angle, and differences in composition of the standards used to compare with the unknown samples.

When the electron beam ionizes inner atomic shells and these ionizations cause the emission of characteristic X-rays, secondary fluorescence can occur, originating from ionizations induced by X-ray photons produced by the primary electron interactions. This fluorescence enhancement effect occurs when an atom species present in the target has an inner-shell ionization energy lower than the energy of other characteristic X-rays or bremsstrahlung photons that originate within the sample. In such a case, the measured X-ray intensity from the fluoresced element will include both the direct electron-excited intensity as well as the additional intensity generated by such enhancement. Despite there exist many approaches available for the assessment of fluorescence enhancement (Reed, 1965; Ugarte et al., 1987), it is impossible to compare these predictions with experimental data as the photons produced by fluoresced atoms cannot be discriminated from the total recorded radiation. Therefore, Monte Carlo simulations constitute a very important tool for estimating the fluorescence enhancement and a number of

Received September 10, 2014; accepted March 26, 2015
*Corresponding author. gcas@famaf.unc.edu.ar

specific situations have been faced with this approach (Fisher, 1971; Hu & Pan, 2001; Llovet & Galan, 2003; Fournelle et al., 2005; Fournelle, 2007).

When performing Monte Carlo simulations of radiation transport, a particle track is pictured as a sequence of stochastic free steps, each ending in an interaction, which changes its direction of movement and its energy, and also may produce secondary particles. The probabilities governing each interaction are associated with the corresponding total and differential cross-sections, which allow to determine the free path between successive interactions, the type of interaction taking place, and the particle energy loss and angular deflection. If the number of generated tracks is large enough, quantitative information on the transport process may be obtained by averaging over a statistically significant number of trajectories. In this work, the PENELOPE routine package (Salvat et al., 2009) has been chosen as it has proved to adequately describe EPMA experimental situations (Acosta et al., 1998; Llovet et al., 2003; Salvat et al., 2006; Escuder et al., 2008, 2010).

It is important to note that, as the ionization cross-sections are quite small for both electrons and photons, secondary fluorescence is very unlikely, because it involves two ionization processes. Variance reduction techniques allow to achieve better statistical uncertainties, without an exaggerated increase of CPU time. In the so-called *splitting technique* (Kahn & Harris, 1951) used here, it is assumed that primary particles start moving with unit statistical weight and each secondary particle produced by a primary one is assigned an initial weight equal to that of the primary. Splitting is also offered by the PENELOPE package and consists of transforming some particles of interest into a number NSPLIT > 1 of identical particles in the same state. In order to leave the simulation results unbiased, weights are assigned to these particles: each particle of interest, originally with a weight w_o, is replaced by NSPLIT copies assigned with weights $w = w_o/$ NSPLIT (Salvat et al., 2009). Another method for variance reduction is called *interaction forcing* (Bielajew & Rogers, 1988), particularly efficient for the simulation of X-ray spectra. However, for fluorescence enhancement simulation, it is not as suitable as the splitting technique chosen here. The implementation of *interaction forcing* in the PENELOPE package favors all ionization processes for a particle kind (electrons or photons), which consumes CPU time in events nonrelated with the phenomenon under study, for example, L-shell ionizations instead of K-shell ionizations. On the other hand, splitting readily allows the specific selection of the photons involved in the process of interest.

In this work, characteristic secondary fluorescence enhancement in EPMA has been studied by using the splitting alternative offered by PENELOPE. As the primary intensity I_p directly generated by the electron beam is enhanced by the secondary intensity I_s, corresponding to ionizations produced by other photons present in the sample, the fluorescence correction factor F is computed as

$$F = 1 + \frac{I_s}{I_p}. \quad (1)$$

In order to analyze the dependence of the statistical uncertainties of F with the NSPLIT parameter, the secondary intensity I_s was studied for different compositions in Fe–Ni binary alloys. This combination of elements was chosen to bring to evidence the fluorescence enhancement effect as both Ni-Kα and Ni-Kβ photons can ionize the Fe-K shell. Three typical incident energies (10, 15, and 20 keV) were selected in order to perform the assessments, for each of which the NSPLIT values ranged from 10 to 10,000.

Materials and Methods

The main program PENSLAB was modified from the PENELOPE 2003 distribution to take into account the different characteristic enhancements; this new code is called PENFLUO and was updated to fulfill the PENELOPE 2008 requirements. In particular, PENFLUO involves all secondary fluorescence by taking advantage of the splitting variance reduction technique offered by the 2008 distribution. Several attempts have been made for the simulation of different EPMA experiments (Llovet et al., 2005, 2014; Salvat et al., 2007; Bote et al., 2008), all of them taking advantage of the capabilities of the geometry subroutine package PENGEOM; this results particularly useful for the simulation of particles, multilayer samples, and a variety of interfaces. For homogeneous flat samples, as those considered in this work, the efficiencies of these programs for the assessment of the fluorescence enhancements are rather low. Instead, the modifications introduced to this aim in the PENSLAB program avoid all the CPU time that PENGEOM devotes to compute distances to the quadric surfaces involved in the geometry definition.

When an electron hits the sample a shower starts, the electrons from the beam are simulated first, while second-generation particles are saved into a stack, then the simulation of second-generation particles begins: once the primary track is completed, the program classifies the photons into Ni-Kα or Ni-Kβ, and then they are cloned, by calling the VSPLIT routine, that is, an integer number (NSPLIT) of photons are created in the same initial conditions. When Fe characteristic photons (third-generation particles) are produced by these second-generation photons, they are classified according to the different possibilities for secondary fluorescence: Fe-Kα by Ni-Kα, Fe-Kα by Ni-Kβ, Fe-Kβ by Ni-Kα, and Fe-Kβ by Ni-Kβ. In order to make PENFLUO carry out this classification, the fifth component in the array of particle labels ILB was used to store the information corresponding to the process which originated second- and third-generation particles (Salvat et al., 2009). Each secondary X-ray distribution is finally stored in counter arrays, which are sent to separate output files. As mentioned in the introduction, all the computed distributions are normalized by NSPLIT in order to not bias the results.

Results are then compared for different choices of NSPLIT, whose values were tested between 10 and 10,000. It is worth emphasizing that the splitting technique is used here to reduce the statistical errors in I_s, as they bear higher uncertainties than

I_p; however, splitting is not appropriate to reduce the I_p uncertainties in the case of low Fe concentration, where the fluorescence correction is most important, as most CPU time is devoted to the simulation of Ni-K photons (NSPLIT copies). In order to fully perform the assessment of the factor F, additional simulations with no splitting (NSPLIT = 1) must be run to achieve appropriate statistical errors.

The adopted values for the simulation parameters were chosen to take advantage of the CPU time for simulating electrons above the Fe inner-shell ionization energy (E_{abs} = 7.11 keV), and photons slightly below the Fe-Kα characteristic energy (E_{abs} = 6.399 keV). The choice of the remaining parameters was $C_1 = 0.05$, $C_2 = 0.05$, W_{cc} = 100 eV, and W_{cr} = 100 eV.

All the simulations for secondary fluorescence distributions were run in an Intel® (Santa Clara, California, USA) Quad CPU Q8400 @ 2.66 GHz processor during 24 h in order to bring to evidence the influence of NSPLIT in the resulting statistical uncertainties for a fixed CPU time. In the case of the simulation of "primary" Fe X-rays, a higher CPU time of 96 h was required.

Results and Discussion

The predicted fluorescence enhancement bears the expected behavior as a function of the concentration of the element of interest. This is exemplified in Figure 1, in which the F results for NSPLIT = 100 are compared with the prediction of the corrected Reed's model of Venosta & Castellano (2013). As shown in this reference, the original Reed's model provides an 11% overestimation in the fluorescence correction factor by assigning 100% Kα yield. Therefore, the few percent differences between the present simulated F values and the modified Reed's model are expectable in view of all the approximations involved in both the original and corrected algorithms. It is worth emphasizing that in the most sensitive case of 1% Fe, these differences would imply a correction of 500 ppm (0.05%).

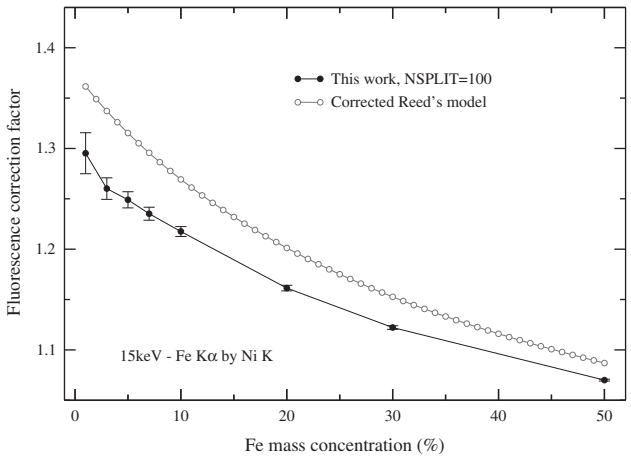

Figure 1. Comparison of the present Monte Carlo simulation for the fluorescence correction factor with the modified Reed's model of Venosta & Castellano (2013) for an electron beam energy of 15 keV as a function of Fe mass concentration.

All possible enhancements for 10 keV are displayed in Figure 2, in which the curves obtained for different NSPLIT values are shown for each enhancement situation. In order to not hinder the comparisons, only error bars for NSPLIT = 10 and 100 are displayed. It becomes evident that the higher the splitting effect, the lower the fluctuations are for each curve, a behavior observed in all the simulations performed along this work. It can also be seen that for enhancements with low probabilities, the statistical uncertainties consequently increase, as explained below.

It is important to notice that the F factor increases when the Fe concentration decreases, but also the absolute and relative uncertainties increase for lower Fe concentrations. The evaluation of F involves the assessment of the secondary intensities, for which the relative statistical uncertainties are expected to decrease as the parameter NSPLIT increases. This behavior can be analyzed by means of the efficiency of the Monte Carlo algorithm (Salvat et al., 2009), which relates the CPU time T for which the simulation produces an estimate $\overline{f}$ for the magnitude of interest with a statistical uncertainty σ_f:

$$\epsilon = \frac{1}{T}\left(\frac{\overline{f}}{\sigma_f}\right)^2.$$

In the limit of large number of showers N, σ_f^2 and T are proportional to $1/N$ and N, respectively, and therefore ϵ is independent of N. Clearly, for fixed T (large enough), a high value for ϵ is a measure of how small the relative uncertainty $(\sigma_f/\overline{f})$ is. Figure 3 shows the behavior obtained for ϵ as a function of Fe concentration, in the case of Fe-Kα secondary intensity induced by Ni-Kα for 15 keV beam electrons, with different choices of the NSPLIT parameter. As expected, ϵ increases with NSPLIT, evidencing that the relative errors are being reduced. It can also be seen that increasing NSPLIT in one order of magnitude translates in an order of magnitude gain in ϵ, up to NSPLIT = 1,000, above which the improvement becomes smaller.

The trend observed for ϵ (and therefore for the relative uncertainties) can be inferred from the dependence of the secondary intensities produced at fixed CPU time. As an example for 20 keV beam energy, Figure 4 shows that the Fe-Kα secondary intensity induced by Ni-Kα mainly grows with the Fe concentration in the range of study—similar trends have been obtained for all beam energies and all enhancements. Although the Ni concentration reduces, and consequently the number of Ni fluorescing photons, a higher number of Fe atoms are present in the sample; as Ni-K photons are quite efficient for ionizing Fe, the result in this competition is an increase in the secondary intensity. This is the behavior exhibited in the plot up to certain Fe concentration, from which a slight decay in the secondary intensity is observed.

In view of the statistical nature of the uncertainties in the secondary intensities, the corresponding relative errors are expected to decrease with increasing scoring. From Figure 4,

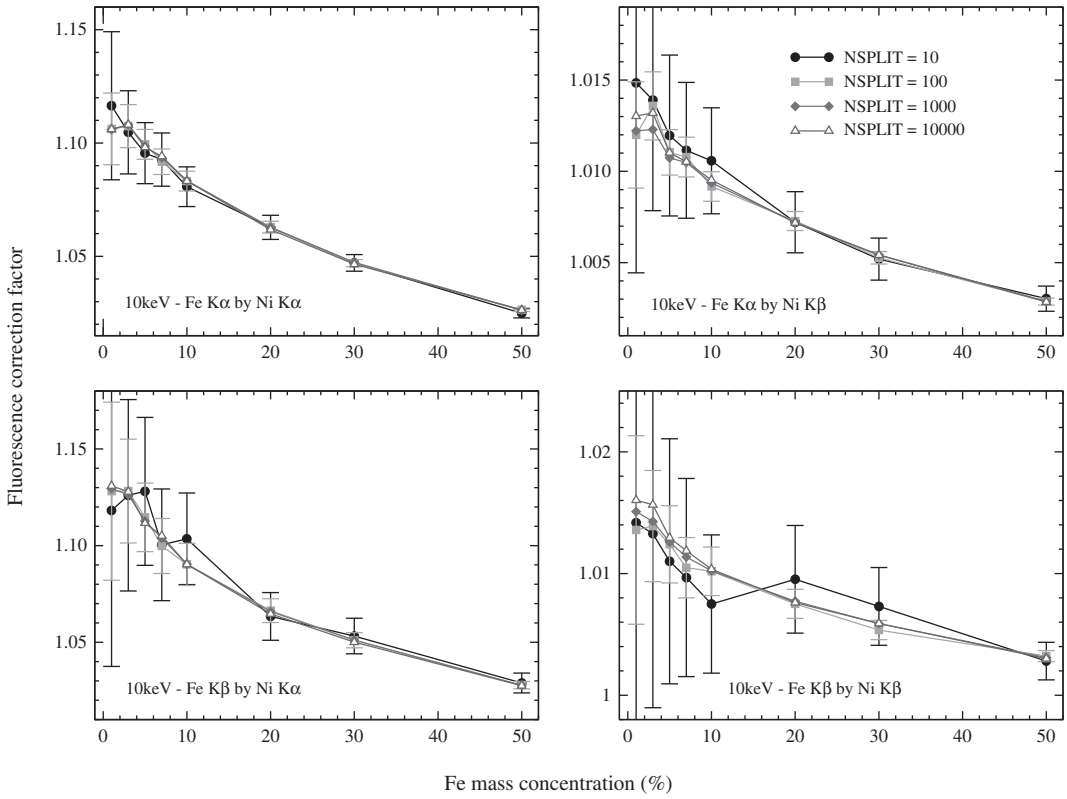

Figure 2. Fluorescence correction factor for an electron beam energy of 10 keV as a function of Fe mass concentration: Fe-Kα by Ni-Kα, Fe-Kα by Ni-Kβ, Fe-Kβ by Ni-Kα, and Fe-Kβ by Ni-Kβ. Only error bars for NSPLIT 10 and 100 are displayed.

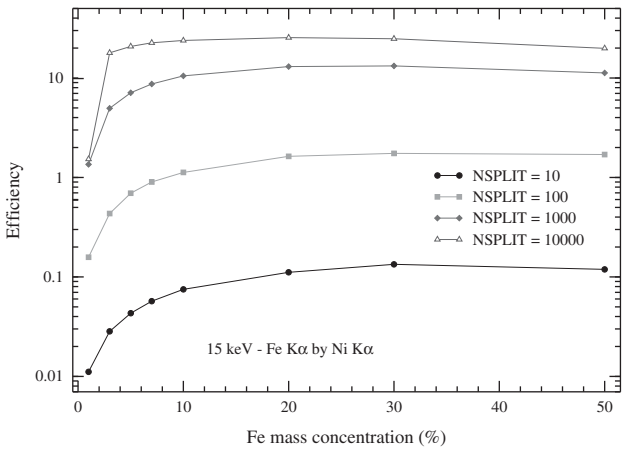

Figure 3. Efficiency of the Monte Carlo algorithm for the assessment of Fe-Kα secondary intensity induced by Ni-Kα as a function of Fe concentration for 15 keV incident electrons for different NSPLIT values.

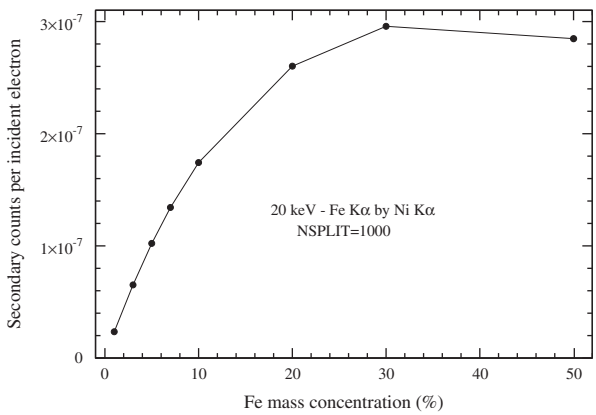

Figure 4. Fe-Kα secondary intensity enhanced by Ni-Kα as a function of Fe mass concentration for beam electrons of 20 keV.

it is clear that, as Fe concentration increases, more secondary events are registered, which means better statistics, and consequently, smaller relative errors; this is reflected in Figure 5 for the particular case of Fe-Kβ intensity enhanced by Ni-Kα photons for a beam energy of 10 keV.

It is also important to note that, for the process under study, when the NSPLIT parameter increases, better statistics is achieved up to a certain level beyond which the extremely high number of split photons prevents from attaining a reasonable survey in the number of showers: the physical situation of almost isotropic characteristic emission originating in the diffusion of beam electrons would not be reproduced. In addition, extremely high values of NSPLIT may also lead to underflow round-off errors when the tallies are incremented with vanishing contributions owing to exceedingly small statistical weights. It becomes clear that choosing exaggerate values for NSPLIT may distort some of

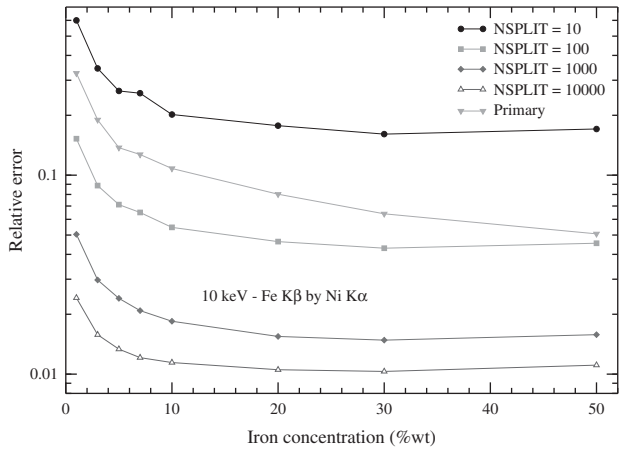

Figure 5. Relative errors for Fe-Kβ intensity enhanced by Ni-Kα at 10 keV as a function of Fe concentration for different NSPLIT values. Uncertainties for primary Fe-Kβ intensity are also shown for comparison.

the produced distributions without a noticeable reduction in the uncertainties.

It must be emphasized that the fluorescence enhancement is finally assessed by computing the F factor given by equation (1). Evidently, by increasing NSPLIT, the uncertainties σ_s in I_s are reduced and the errors in F

$$\sigma_F = (F-1)\sqrt{\left(\frac{\sigma_p}{I_p}\right)^2 + \left(\frac{\sigma_s}{I_s}\right)^2},$$

are governed by the uncertainties σ_p in I_p. In the particular enhancement shown in Figure 5, it is clear that this situation occurs when choosing NSPLIT $\geq$ 100. It is therefore convenient to choose an NSPLIT value high enough and perform a separate (NSPLIT = 1) simulation for the primary intensity with reasonable statistics. As mentioned in the Materials and Methods section, in the present assessment of primary Fe X-rays a CPU time of 96 h was chosen.

Conclusions

A Monte Carlo code was developed for the simulation of the characteristic secondary fluorescence enhancement in EPMA, by modifying the main program PENSLAB provided in the PENELOPE 2003 distribution, and finally updated to fulfill the PENELOPE 2008 requirements. This program allows to assess all secondary characteristic enhancement by taking advantage of the splitting variance reduction technique. Third-generation photons are classified through the fifth component in the array of particle labels ILB, according to the process which gives rise to this enhancement effect (Salvat et al., 2009).

The characteristic fluorescence enhancement has been simulated using several NSPLIT values for Fe–Ni alloys of different compositions. The efficiencies for the simulated secondary intensities bear a remarkable improvement when increasing the NSPLIT parameter; although in most cases an NSPLIT value of 100 is sufficient, some less likely enhancements may require stronger splitting in order to increase the efficiency associated with the simulation of secondary intensities.

Although interaction forcing is a variance reduction technique, particularly efficient for reproducing X-ray spectra, for characteristic fluorescence enhancement simulation it is not as suitable as the splitting technique chosen here, as explained above. It may, however, be useful for analyzing the bremsstrahlung enhancement, as all the radiative interactions are favored and all the continuum photons with energies above the binding energy of the fluoresced atoms are involved in this process. This will be the subject of investigation in near future.

Acknowledgment

The authors wish to thank the *Secretaría de Ciencia y Técnica* of the *Unversidad Nacional de Córdoba.*

References

Acosta, E., Llovet, X., Coleoni, E., Riveros, J.A. & Salvat, F. (1998). Monte Carlo simulation of x-ray emission by kilovolt electron bombardment. *J Appl Phys* **83**, 6038–6049.

Bielajew, A. & Rogers, D. (1988). Variance-reduction techniques. In *Monte Carlo Transport of Electrons and Photons* (Ettore Majorana International Science Series, vol. 38, T. Jenkins, W. Nelson & A. Rindi (Eds.), pp. 407–419. New York, NY: Plenum Press.

Bote, D., Llovet, X. & Salvat, F. (2008). Monte Carlo simulation of characteristic x-ray emission from thick samples bombarded by kiloelectronvolt electrons. *J Phys D Appl Phys* **41**, 105304.

Escuder, J.A., Llovet, X. & Salvat, F. (2008). Numerical calculation of secondary fluorescence effects near phase boundaries in EPMA. *Microsc Microanal* **14**(Suppl 2), 126–127.

Escuder, J.A., Salvat, F., Llovet, X. & Donovan, J.J. (2010). Numerical correction for secondary fluorescence across phase boundaries in EPMA. *IOP Conf Ser Mater Sci Eng* **7**, 012008.

Fisher, G.L. (1971). An investigation of electron probe microanalysis corrections in nickel-cobalt alloys. *J Phys D Appl Phys* **4**, 1439–1447.

Fournelle, J.H. (2007). The problem of secondary fluorescence in EPMA in the application of the Ti-in-zircon geothermometer and the utility of PENEPMA Monte Carlo Program. *Microsc Microanal* **13**(Suppl 2), 1390 CD.

Fournelle, J.H., Kim, S. & Perepezko, J.H. (2005). Monte Carlo simulation of Nb Kα secondary fluorescence in EPMA: Comparison of PENELOPE simulations with experimental results. *Surf Interface Anal* **37**, 1012–1016.

Goldstein, J., Newbury, D., Joy, D., Lyman, C., Etchling, P., Lifshin, E., Sawyer, L. & Michael, J. (2003). *Scanning Electron Microscopy and X-Ray Microanalysis*, 3rd ed. New York, NY: Kluwer Academic/Plenum Publishers.

Hu, Y. & Pan, Y. (2001). Method for the calculation of the chemical composition of a thin film by Monte Carlo simulation and electron probe microanalysis. *X-Ray Spectrom* **30**, 110–115.

Kahn, H. & Harris, T.E. (1951). Estimation of particle transmission by random sampling. *Natl Bur Stand Appl Math Ser* **12**, 27–30.

Llovet, X., Fernández-Varea, J.M., Sempau, J. & Salvat, F. (2005). Monte Carlo simulation of X-ray emission using the general-purpose code PENELOPE. *Surf Interface Anal* **37**, 1054–1058.

Llovet, X. & Galan, G. (2003). Correction of secondary X-ray fluorescence near grain boundaries in electron microprobe analysis: Application to thermobarometry of spinel lherzolites. *Am Mineral* **88**, 121–130.

Llovet, X., Pinard, P.T. & Salvat, F. (2014). Application of Monte Carlo calculations to improve quantitative electron probe. *Microsc Microanal* **20**(Suppl 3), 708–709.

Llovet, X., Sorbier, L., Campos, C.S., Acosta, E. & Salvat, F. (2003). Monte Carlo simulation of X-ray spectra generated by kilo-electron-volt electrons. *J Appl Phys* **93**, 3844–3851.

Reed, S.J.B. (1965). Characteristic fluorescence corrections in electron-probe microanalysis. *Br J Appl Phys* **16**, 913–926.

Reed, S.J.B. (1993). *Electron Probe Microanalysis*, 2nd ed. Cambridge: Cambridge University Press.

Salvat, F., Escuder, J.A., Bote, D. & Llovet, X. (2007). Simulation of EPMA spectra using PENELOPE. *Microsc Microanal* **13**(Suppl 2), 1388–1389.

Salvat, F., Fernández-Varea, J.M. & Sempau, J. (2009). *PENELOPE-2008, a Code System for Monte Carlo Simulation of Electron and Photon Transport*. Issy-les-Moulineaux, France: OECD Nuclear Energy Agency.

Salvat, F., Llovet, X., Fernández-Varea, J.M. & Sempau, J. (2006). Monte Carlo simulation in electron probe microanalysis. Comparison of different simulation algorithms. *Microchim Acta* **155**, 67–74.

Scott, V., Love, G. & Reed, S. (1995). *Quantitative Electron-Probe Microanalysis*, 2nd ed. New York, NY: Ellis Horwood Ltd.

Ugarte, D., Castellano, G., Trincavelli, J., del Giorgio, M. & Riveros, J.A. (1987). Evaluation of the main atomic number, absorption and fluorescence correction models in quantitative microanalysis. *X-Ray Spectrom* **16**, 249–254.

Venosta, L. & Castellano, G. (2013). Separate K-line contributions to fluorescence enhancement in electron probe microanalysis. *Spectrochim Acta Part B* **81**, 59–63.